Comprehensive Structural Studies of 2′,3′-Difluorinated Nucleosides: Comparison of Theory, Solution, and Solid State

ARTICLE *in* JOURNAL OF THE AMERICAN CHEMICAL SOCIETY · AUGUST 2008

Impact Factor: 12.11 · DOI: 10.1021/ja800964g · Source: PubMed

Published in final edited form as:
J Am Chem Soc. 2008 July 16; 130(28): 9048–9057. doi:10.1021/ja800964g.

Comprehensive Structural Studies of 2′,3′-Difluorinated Nucleosides: Comparison of Theory, Solution, and Solid State

Joseph J. Barchi Jr.[*], **Rajeshri G. Karki**[†], **Marc C. Nicklaus**, **Maqbool A. Siddiqui**, **Clifford George**[‡], **Igor A. Mikhailopulo**[§], and **Victor E. Marquez**
Laboratory of Medicinal Chemistry, National Cancer Institute, Frederick, National Institutes of Health, 376 Boyles Street, P.O. Box B, Frederick, Maryland 21702

Abstract

The conformations of three 2′,3′-difluoro uridine nucleosides were studied by X-ray crystallography, NMR spectroscopy, and ab initio calculations in an attempt to define the roles that the two vicinal fluorine atoms play in the puckering preferences of the furanose ring. Two of the compounds examined contained fluorine atoms in either the *arabino* or *xylo* dispositions at C2′ and C3′ of a 2′, 3′-dideoxyuridine system. The third compound also incorporated fluorine atoms in the *xylo* configuration on the furanose ring but was substituted with a 6-azauracil base in place of uracil. A battery of NMR experiments in D_2O solution was used to identify conformational preferences primarily from coupling constant and NOE data. Both ^1H and ^{19}F NMR data were used to ascertain the preferred sugar pucker of the furanose ring through the use of the program PSEUROT. Compound-dependent parameters used in the PSEUROT calculations were newly derived from complete sets of conformations calculated from high-level ab initio methods. The solution and theoretical data were compared to the conformations of each molecule in the solid state. It was shown that both gauche and antiperiplanar effects may be operative to maintain a pseudodiaxial arrangement of the C2′and C3′ vicinal fluorine atoms. These data, along with previously reported data by us and others concerning monofluorinated nucleoside conformations, were used to propose a model of how fluorine influences different aspects of nucleoside conformations.

Introduction

The use of fluorine as a surrogate for either hydrogen or a hydroxyl group has a long and prosperous history in drug design and discovery.[1] The highly electronegative nature of the fluorine atom imparts very different electrostatic properties to a molecule, and this effect may in turn influence the conformation of the system to which it has been incorporated in unique ways. These distinct changes are installed without major disturbances to the steric properties of the molecule due to the small size and high “compactness” of the fluorine. For this reason, fluorine has been considered to be a suitable bioisostere for hydrogen. In addition, the electronegative properties of fluorine, along with its capability to accept a hydrogen bond, make it a near “isoelectronic” replacement for the hydroxyl group. These postulates have been borne out empirically: There are countless examples of the biological utility of functional group

E-mail: barchi@helix.nih.gov.
[†]Present address: Global Discovery Chemistry-CADD, Novartis Institutes for Biomedical Research, Inc., 3160/100 Technology Square, Cambridge, MA 02139.
[‡]Naval Research Laboratory, Washington, DC, Retired from service.
[§]Institute of Bioorganic Chemistry, National Academy of Sciences of Belarus, 220141 mink, Acad. Kuprevicha 5/2 Belarus.

Supporting Information Available: Table of physical data for compounds **2**–**4**, graphs of torsion angle plots for A/B coefficient calculations, table of all A/B coefficients, Cartesian coordinates for ab initio-optimized structures, CIF files for compounds **2**–**4** and numbering scheme used in CIF files. This material is available free of charge via the Internet at http://pubs.acs.org.

replacement by fluorine, and this substitution often yields active therapeutic candidates with modified biophysical properties.[2] Replacement of a hydroxyl group with a fluorine atom usually results in a more lipophilic molecule and thus may yield compounds with enhanced membrane permeability and more favorable pharmacokinetic properties.[3]

The synthesis of both nucleoside and nucleotide analogues via atom substitution with fluorine has also been a recurring theme in the literature for the past 25 years. In fact, virtually every hydrogen atom or hydroxyl group from the known endogenous nucleosides has been replaced with fluorine via either single- or multiple-atom substitutions. Many of these novel agents exhibit modified biological potency compared with the parent compounds. After the discovery that azidothymidine (AZT) and other 2′,3′-dideoxy nucleosides had potent anti-HIV activity (primarily through inhibition of viral reverse transcriptase, RT), dideoxy nucleosides containing a single fluorine substitution were rapidly evaluated as anti-HIV agents and many were found to be potent analogues.[4,5] Several examples have come out of this laboratory, most notably the acid-stable adenosine analogue Lodenosine (**1**, Chart 1), a second-generation RT inhibitor that was taken to phase 1 clinical trials.[6-8]

The complete compendium of fluorinated (and other) nucleoside derivatives has been critically evaluated over the past several years in an attempt to accurately relate structural features with the wide-ranging differences observed in activity profiles. The structural features that may be altered by the presence of fluorine are those that define the nucleosides template: (1) the conformation of the furanose ring as defined by the concept of pseudorotation[9] (Figure 1, center) which is described by the two pseudorotation parameters *P* (the phase angle of pseudorotation) and ν_{max} (Figure 1B, the maximum out-of-plane pucker of the ring corresponding to the radius of the circle); (2) the glycosyl rotamer angle χ (Figure 1A and C) and (3) the C4′–C5′ bond rotamer angle γ (Figure 1A and D). In the early 1990s, a survey of the crystal structures of known anti-HIV active nucleosides revealed that their furanose rings puckered in the Southern (*S*) hemisphere ($P \approx 180°$), whereas those of inactive compounds crystallized in the Northern (*N*) hemisphere ($P \approx 0°$).[10] A notable exception was the C2′–C3′ unsaturated thymidine analogue stavudine, whose nearly flat furanose ring was shown to be virtually devoid of any out-of-plane puckering;[11] other investigators have also countered the "*S* = active" argument.[12]

The distinct impact on the conformation of the furanose system when substituted at either C2′ or C3′ with electronegative fluorine has primarily been attributed to the gauche effect (GE) [13,14] between the fluorine and the O4′ oxygen atom.[15] An alternative theory that has been invoked to describe the specific arrangements of atoms on a furanose ring,[16-18] coined the antiperiplanar effect (AP),[19] purports that the most electronegative atoms will prefer to be anti with the least electronegative atoms, and the ring substituents will attempt to "maximize" the number of these arrangements in a particular structure. These, along with the anomeric effect (AE), all contribute to the specific ring pucker of furanose ring-substituted nucleosides.

Figure 2 depicts the potential GE and AE conformations that may be populated with two vicinal, trans C2′,C3′ fluorine atoms. The successful design of biologically active nucleosides by a single fluorine substitution in the furanose ring prompted the examination of difluorinated derivatives. In particular, the synthesis of molecules that incorporate fluorines with the configurations at C2′ and C3′ that will allow the aforementioned electronic effects to work in concert to favor the active "*S*" (C2′-*endo*, C3′-*exo*) sugar pucker (vide supra) should intuitively produce active anti-HIV compounds. It was shown however, that this was not the case regarding compound **2** (Chart 1) when we and others previously studied the pseudorotational equilibrium and anti-HIV-1 activity of difluoro nucleosides.[20] Hence, we decide to explore the structural details that may have contributed to the lack of anti-HIV activity of compounds **2**–**4** shown in Chart 1. One question to answer was whether the F–F gauche (or other) effects would override

other stereoelectronic effects to yield "unpredictable" ring puckers. In addition we wished to gain more insight into the potential "up"-F3′–H6 interaction previously observed by Bergstrom (vide infra).[21] This group postulated that the conformation of pyrimidine nucleosides with fluorine substitution in the C3′-*endo* position may influence the furanose ring pucker through a hydrogen bond with the H6 proton.

Materials and Methods

Synthesis

The *arabino*-difluoronucleoside **2** (*arabino*-FF) was synthesized according to the method of Martin, et al.[22] and by a separate method (Siddiqui and Marquez, unpublished). The *xylo*-difluoro nucleosides **3** (*xylo*-FF) and **4** (*6Nxylo*-FF) used in this study were synthesized previously in this laboratory.[20]

X-ray Crystallography

Data collection was performed with a Bruker SMART[23] 6K CCD detector on a Platform goniometer. The Rigaku rotating Cu anode source was equipped with incident beam Göbel mirrors. Lattice parameters were determined using SAINT[23] from 4589 reflections within 4.4° < 2θ < 129.56° (compound **2**), 4589 reflections within 4.4° < 2θ < 129.56° (compound **3**) or from 2292 reflections within 9.0° < 2θ < 134.1° (compound **4**). The data collection range had a (sin θ)/λ_{max} = 0.59–0.60. A set of reflections (total/unique: 5047/1772 (**2**), 14 03/3500 (**3**), 2515/1357 (**4**)) was collected in the ω scan mode. Corrections were applied for Lorentz, polarization, and absorption effects. The structures were solved with SHELXTL and refined with the aid of the SHELX97[24] system of programs. The full-matrix least-squares refinement on F^2 varied 161 (**2** and **4**) or 410 (**3**) parameters and included 16 restraints: atom coordinates, and anisotropic thermal parameters for all non-H atoms. H atoms were included using a riding model [coordinate shifts of C applied to attached H atoms, C–H distances set to 0.96–0.93 Å, H angles idealized, U_{iso}(H) were set to 1.2–1.5 U_{eq}(C). Final residuals were as follows. Compound **2**, $R1$ = 0.041 for the 1668 observed data with $F_o > 4\sigma(F_o)$ and 0.039 for all data; Compound **3**, $R1$ = 0.044 for the 2703 observed data with $F_o > 4\sigma(F_o)$ and 0.029 for all data; Compound **4**, $R1$ = 0.030 for the 1332 observed data with $F_o > 4\sigma(F_o)$ and 0.031 for all data.

Computational Methods

Using the experimentally determined crystal structure as a starting point, the structures of **2**–**4** were energy minimized using the Merck Molecular Force Field (MMFF)[25] and a continuum solvation model for H_2O[26] in Macromodel (version 8.0, Schrödinger LLC, New York). The minimized structures were subjected to 1000 steps of Monte Carlo Multiple Minimum (MCMM)[27] conformational search routine. All conformers within 20 kcal/mol of the global energy minimum were saved. The lowest energy conformation for each molecule obtained by MCMM simulations were next subjected to full optimization in the gas phase using Gaussian98[28] (version A11) at the RHF/6-31G* (DFT) level. This was followed by three more optimization steps: (1) B3LYP/6-31G* level of theory, (2) a single-point energy calculation at the B3LYP/6-311++G** level, and (3) full optimization at B3LYP/6-311++G.

Prediction of NMR Shift for the Optimized Structures

Structures of **2**–**4** were optimized by constraining the v_0 (C4′–O4′–C1′–C2′) and v_3 (C2′–C3′–C4′–O4′) values to obtain desired values of P and v_{max} (Figure 1). Starting from these partially optimized structures, all compounds were completely optimized at the AM1 level followed by increasing levels of theory (RHF/6-31G* then B3LYP/6-31G* then B3LYP/6-311++G**). For each nucleoside, two geometries were optimized: one with P = 0° (north) and another with P = 180° (south). These structures were then used for predicting NMR chemical shielding effects.

TMS and $CFCl_3$ were used as reference standards for (C,H) and F, respectively. The standards were also optimized in the same manner as the nucleosides above. NMR chemical shielding values were evaluated employing the gauge-independent atomic orbital (GIAO)[29] method at the B3LYP/6-311++G** optimized geometry. All calculations were done using Gaussian98 A11. The calculated NMR chemical shifts (δ) were then obtained using the formula:

$$\delta(i) = \delta(a) - \delta(b)$$

where *i* is the atom under consideration, $\delta(a)$ is the calculated chemical shielding of the reference atom, and $\delta(b)$ is the calculated chemical shielding of the atom under consideration. The frequency calculation for the optimized structure showed no negative frequencies. Calculations utilized the high-performance computational capabilities of the Biowulf/LoBoS3 cluster at the National Institutes of Health, Bethesda, MD.

NMR Studies

NMR spectra of **2**–**4** were obtained at 500 MHz on a Varian INOVA instrument. Data were collected using either a triple resonance H,C,N (^{1}H S/N > 1000:1) or an H–F probe designed by Nalorac/Varian. The H–F probe was equipped for full observe or decoupling capabilities for either the ^{1}H or ^{19}F frequencies. Temperature control achieved by heating of dry nitrogen gas (dew point −40 °C FTS400 cooler) with the Varian temperature control unit. Samples were between 5 and 15 mM in D_2O and were unbuffered. One-dimensional proton spectra were acquired at temperatures from 10 to 70 °C in 15 °C increments with 64k data points, a sweep width of 4000 Hz (acquisition time of 8 s) and were zero-filled to 131 912 points. Resolution enhancement was provided by Gaussian multiplication. Data were referenced to D_2O at 4.65 ppm (chemical shift changes with temperature were not an issue since the primary concerns were changes in coupling constants). Fluorine 1D spectra were obtained at 470.176 MHz with a sweep width and 10 000 Hz and an acquisition time of 2 s. Fluorine chemical shifts are reported relative to fluorotrichloromethane ($CFCl_3$, fluoroform) at 0.0 ppm. Fluorine-decoupled ^{1}H(^{19}F) spectra were obtained with either with WURST[30] adiabatic (broadband) decoupling scheme or with selective decoupling of a specific ^{19}F resonance using an i-SNOB[31] shaped pulse. Proton–fluorine NOE spectra were obtained with a modified HOESY sequence (Varian pulse sequence HOESY.c supplied in the user sequence library at www.varianinc.com). One-dimensional ^{1}H–^{1}H NOE spectra were obtained by the method of Shaka et al.[32] (DPFGSE sequence in the Varian CHEMPACK pulse sequence library), with a preacquisition delay of 5 s using a selective pulse on the irradiated resonance.

Coupling Constant Analysis

Most ^{1}H–^{1}H *J* values were derived from the resolution-enhanced 1D spectra. For complex spin system with second order effects, simulations using the gNMR program (Adept Scientific) were employed. The eight spin system (six protons for H1′–H5″and two F atoms) was simulated by exact input of chemical shifts for the furanose ring protons and addition of the fluorine nuclei was made by placing the ^{19}F chemical shifts 100 ppm upfield of the most shielded proton spin (^{19}F signals were placed at the relative positions that they appeared in the experimental spectrum). For each spectrum, a “best fit” approach was initially performed to obtain a spectrum that closely matched the experimental data. This was followed by fitting each spectral transition from the imported experimental spectrum with the simulated data via the iteration utility in gNMR. Final *J* values were taken from the simulated data that best matched the experimental spectrum. The most accurate ^{1}H–^{19}F *J* values were also obtained by similar spectral simulation and optimization in gNMR.

PSEUROT Analysis

The N ↔ dynamic equilibrium was studied with the program PSEUROT v.6.3 (supplied by Prof. Cornelis Altona, University of Leiden, The Netherlands). Several different starting parameters were used to comprehensively explore the conformational space sampled by the compounds. All PSEUROT calculations were performed such as to achieving the minimal rms deviations and $|\Delta J|$ values. The FLUOROT version of the program that has been parametrerized for inclusion of J_{HF} data[33] was used for comparison of calculations with either or both $J_{H,H}$ and $J_{H,F}$ data. Scale factors for $^3J_{(H,H)}$ and $^3J_{(H,F)}$ were 1.0 and 0.2, respectively. It is noteworthy that in the case of arabinoside **2** and xyloside **4** we also used scale factors equal to1.0 for both H–H and H–F couplings and obtained similar pseudorotational parameters (see Table 5). The A_j and B_j values used were those calculated from the geometries obtained from the ab initio studies (see below and Supporting Information). The value of v_{max} varied between 36°and 44°and was largely held constant during the calculations. The electronegativities of various substituents were those found in the database file of the PSEUROT program with fluorine set to 1.37.

Determination of Coefficients *A* and *B*

The *A* and *B* coefficients were determined from the optimized structures of **2**–**4** that were obtained from the quantum mechanical calculations. A series of 24 structures corresponding to *P* values ranging between 0 and 345 in increments of 15° with v_{max} = 30° were generated using Insight II (Accelrys, Inc.). The crystal structures that were completely optimized using Gaussian 98[28] were used as starting points. Constrained optimizations (endocyclic torsion angles v_0 and either v_3 or v_4 were held fixed to maintain conformations with desired values of *P* and v_{max}) were carried out first in a semiempirical mode using AM1 followed by ab initio optimizations similar as described in the Computational Methods section above (RHF/6-31G* ⇒ B3LYP/6-31G* ⇒ B3LYP/6-311++G**). These calculations were repeated with the v_{max} fixed at 38° to compare to data sets with v_{max} values that are typical of standard nucleosides.[34] After optimization, the structures were read into Sybyl 6.8 (Tripos, Inc.) and the various torsion angles measured. The values of the endocyclic torsion angles, *P*, and v_{max} were confirmed using the online pseudorotation tool supplied in the Cactus software (http://cactus.nci.nih.gov/Pseurot). The five endocyclic torsion angles are related to the H–H vicinal torsion angles by the linear relation (eq 1)

$$v_j^{HH} = A_J v_j + B_j \quad j = 0, 1, 2, 3, 4 \tag{1}$$

A plot of the HH torsion against the endocyclic torsions yields a straight line with slope equal to *A* and *y* intercept equal to *B*. All plots from the three nucleosides **2**–**4** (for puckering amplitude values of both 30° and 38°) gave straight lines with correlation coefficients > 0.998 (see Supporting Information).

Results

Synthesis

The synthesis of compound **2** was performed as described by Martin et al.,[21] and that of compounds **3** and **4** according to Marquez, et al.[22] Full characterization data for **2**–**4** (NMR, MS, elemental analysis, melting point) are available in the Supporting Information.

Solid State: X-ray Crystallography

The solid state structures of **2**–**4** and are shown in Figure 3. All of the structures shown represent the absolute configuration for each molecule. While the anomalous X-ray scattering contributions were weak for these small difluoronucleosides, they were sufficient to make an accurate determination of their structures. Table 1 lists the principal structural parameters defining the conformation of these nucleosides.

In **2** (Figure 3A), the (2′*R*, 3′*R*) fluorine atoms in the *arabino* configuration are trans diaxial. The angle γ in this molecule is oriented *synclinal* (-*sc* or γ^{-}; see Figure 1) and the base is anti to the furanose ring. This -*sc* orientation is fixed by intermolecular hydrogen bonding in the unit cell. Both fluorines (2′*R*, 3′*R*) and the 5′-hydroxymethyl group are positioned pseudoaxial to the furanose ring. The uracil base assumes what can be termed as a "pseudobisectional" orientation, i.e, the plane of the heterocyclic ring bisects the plane of the furanose with a χ angle of −142.8°. Compound **2** crystallized with a ring pucker very close to the pure "*S*" form: P = 173.5° is only 6.5° from the $^{2}T_{3}$ (P = 180°) *S* pucker (Figure 1).

Compound **3**, with the two fluorine atoms oriented in the *xylo* configuration and a standard uracil base crystallized with two molecules in the asymmetric unit (conformations **3a** and **3b**) along with a disordered ethanol solvate molecule present at partial occupancy. One of the two asymmetric forms (designated **3b**) is also disordered with the furanose ring present at nearly equal occupancy (45:55, for forms **b** and **b**′) over two positions. In each of the three conformers the orientation of the 5′ OH is γ^{t} (*ap*, antiperiplanar) and the pyrimidine base is oriented anti. The pseudorotation parameter P = 26.5° places the puckering mode near the midpoint between ^{3}E and $^{3}T_{4}$ for the nondisordered molecule **3a** (depicted in Figure 3B) and 6.1° from ^{3}E for conformer **3b** and 4.0° from E_{4} for conformer **3b**′. The γ^{t} (*ap*) orientation of the 5′ OH is fixed in each of the three conformers by intermolecular hydrogen bonds. The (2′*S*, 3′*S*) fluorine ring substituents are pseudoaxial and the base is pseudobisectional (as in **2**), whereas the hydroxymethyl group is pseudoequatorial. In **4**, which differs from **3** by the substitution of nitrogen for C6 in the pyrimidine base, the ring substituents are similarly oriented with respect to the pseudorotational plane. The 5′-$CH_{2}OH$ γ torsion angle, however, differs significantly in value which places the orientation as -*sc*, similar to compound **2**. This orientation is also fixed by a pair of intermolecular hydrogen bonds. Here the hydroxyl acts as both a hydrogen bond donor and acceptor. The P = 55.0° value places the conformation at a near perfect E_{4} envelope (P = 54.0°), not far removed from the ring pucker in all three conformations of **3**.

Theory: ab initio calculations

With the availability of crystal structures, we were able to use these as starting conformations in the several ab initio and molecular dynamics calculations. The three difluoro nucleosides were subjected to rigorous conformational search and analysis using molecular mechanics followed by optimization with ab initio methods. We began with the MMFF followed by extensive conformational searching to locate low-energy structures that were as close as possible to the global minimum. We then concentrated on using these conformations for ab initio calculations to establish a "baseline" of structures based on first principles since there is an extremely small structural database available for compounds containing two vicinal fluorine atoms in nucleoside templates. In addition, we needed a series of low energy structures of various sugar puckers to calculate the coefficients used in the PSEUROT calculations (vide infra) as has been done previously for systems with bond lengths and angles that are possibly distorted from "standard" nucleoside values.[35-37] In addition, we could use ab initio data to qualitatively compare the chemical shifts of proton and fluorine atoms in this small group of vicinal difluoro nucleosides (vide infra).

In general, the ab initio data also confirmed what was observed in the solid and solution states: Through a combination of electronic effects, the sugar pucker for all optimized structures had a tendency for the fluorines atoms to remain pseudoaxial with compound **2** in the *S* hemisphere and **3** and **4** in the northern hemisphere. There were, as would be expected, some distinct differences between the solid state and calculated structures. A comparison of the endocyclic torsion angles and pseudorotational parameters for the solid state and optimum structures calculated by ab initio methods are shown in Table 2. Torsion angle and pseudorotational data for two separate low-energy conformers that were found during the optimization process are depicted in the table. A close examination of the phase angle *P* reveals that for the *arabino*-FF case (**2**), the two calculated conformers remain in the *S* hemisphere but whereas the X-ray structure is almost pure *S*, the two calculated conformers tend more toward the midway point between the "eastern" and "southern" position on the pseudorotational cycle (Figure 1). A higher calculated out-of-plane pucker (v_{max}) positions the base pseudoequatorial, as to be expected for the *S*-conformers. In comparison, the two *xylo*-oriented fluorines in **3** and **4** are also pseudoaxial, and hence the *P* values are in the *N* hemisphere. For **3** with a standard uracil base, the two low-energy conformers are almost identical in torsion values suggestion that this is a global minimum that slightly deviates from the X-ray structure, tending, once again, more toward the eastern hemisphere (*P* angles at ~49°). This could be a consequence of the competing F2′–F3′ GE against the F2′(F3′)–O4 GEs, suggesting that this drives the *P* values away from pure *N*. For the 6*N*-*xylo*-FF compound **4**, the situation is more intriguing, since both the X-ray data and calculated conformer 1 stray significantly from pure *N*, suggesting that the 6-aza nitrogen plays a distinct role in driving the structural parameters of this molecule. The 6-azauracil base tends to be highly pseudoequatorial, most likely owing to the potential repulsive interaction between nitrogen and the 3′-fluorine atom in the more "*N*" type conformers. Calculated conformer 2, however, is essentially pure *N*, with *P* = 0.52°. A provocative aspect of this structure is that the γ angle about the C4′–C5′ bond is rotated to the γ^t quadrant (63°) which positions the 5′-OH in hydrogen bonding proximity with the 6-nitrogen atom of compound **4**. The interplay between the 6-nitrogen of a 6-azauracil base and an *arabino*-oriented fluorine atom in the C2′ position of a nucleoside has been shown to dramatically affect the value of *P*.[38]

Solution Structure: NMR spectroscopy

The three difluoronucleosides were examined exhaustively using a variety of NMR experiments. Both ^{1}H and ^{19}F data were collected and used for calculations of ring pucker by pseudorotational analysis and to compare various parameters with the modeling studies. Data were collected at a series of temperatures ranging from 10 to 70 °C for use in the temperature-dependent calculation of coupling constants and pseudorotational parameters *P* and v_{max} obtained in the PSEUROT program.

NMR data were collected with a maximum number of data points before Fourier transform in an effort to optimally resolve multiplet structure for coupling constant analysis. All of the compounds studied displayed extended coupling networks that ranged from strong two-bond H–F couplings to long-range four-and five-bond couplings between various protons and fluorine, dependent on the stereochemistry of the interacting partners. Taking compound **2** as an example, Figure 4 shows some representative ^{1}H and ^{19}F resonances illustrating the level of resolution obtained. Many resonances were first-order and could be analyzed directly. Hence, it was relatively straightforward to extract several features from these spectra to aid in structural analysis. Tables 3 and 4, respectively, list all HH and HF coupling constants at two extreme temperatures (10 and 70 °C). All multiplets were complicated by coupling to both ^{19}F atoms, but the data were still readily interpretable. For example, several four- and five-bond coupling constants were observed around the furanose ring, viz., $J_{F2',H4'}$, $J_{F3',H1'}$, $J_{F2',H6}$, and $J_{F,H5(H5")}$. Two-bond ^{1}H–^{19}F coupling constants where fluorine is in the C2′ or

C3′ position in nucleosides are generally large (45–55 Hz) and that was the case for compounds **2**–**4**. Figure 4 confirmed that the resonance of the H6 proton on the pyrimidine base was a clean doublet of doublets with the smaller coupling constant attributed to a five-bond interaction between the endo fluorine atom at C2′ and H6. Similar interactions have been observed in other C2′–"up" fluorinated nucleosides in both the pyrimidine[39] and purine[40] families. Other four-bond couplings such as $J_{F2',H4'}$ were seen in all three compounds, indicating either proper geometric arrangement for through bond or through-space coupling.[41]

Although most signals in the NMR were well dispersed, there were still a few complicated multiplets which required additional data for proper analysis. A battery of various NMR experiments and simulation protocols allowed the full analysis of all spectra. Assignment of the fluorine atoms was straightforward, employing selective decoupling of each fluorine or H2′/H3′ resonance using shaped pulses. Perhaps not surprisingly, all fluorine atoms on the endo ("up") side of the nucleosides were shifted upfield from their exo ("down") counterparts with a $\Delta\delta$ of the two fluorine atoms between 13.1 and 15.2 ppm. We confirmed this $\Delta\delta$ by predicting the chemical shifts of all proton and fluorine atoms from ab initio data using the Gauge-Independent Atomic Orbital method[29] as implemented in Gaussian98. We made predictions of the $\Delta\delta$ for two conformers from each of the three difluoro nucleosides fixed in either extreme *N* or *S* puckers, The experimental data were a near exact match for the chemical shifts predicted for the "correct" ring pucker, i.e., between 13 and 14 ppm for the *S* pucker of **2** and the *N* pucker of **3** and **4**, whereas a difference of 3–4 ppm was predicted for the *N* pucker of **2** and the *S* of **3** and **4**.

In order to extract accurate coupling constants for PSEUROT analysis, spectral simulation of all ^{1}H and ^{19}F spectra were performed with the program gNMR (version 5.0, Adept Scientific). It was possible to obtain very accurate data using specific features of gNMR that allowed iterative calculations of *J* values by comparing the actual imported experimental spectrum with the calculated spectrum. Threshold settings allow iterations until a defined "fit" with the experimental spectrum is obtained. In this way, all couplings were calculated with very low error tolerances. An example of the quality of the data is shown in Figure 5 for multiplets from compounds **2** and **4**. Both the ^{1}H and ^{19}F spectra were fit equally well. In addition, several selective decoupling experiments were run for peak assignments, as well as coupling constant calculations via simulations of these "decoupled" spin systems.

Due to the lack of information on bond angles and distances in these vicinal difluoro nucleosides, we required a set of coefficients that relate the furanose endocyclic torsion angles with the exocyclic HH and HF torsions of each molecule (see Materials and Methods). These were obtained from a series of ab initio single-point low-energy structures that were optimized by setting the pseudorotational angle *P* to values that cover the entire 360°of the pseudorotational cycle.[16,34] When these are incorporated into the PSEUROT database, a more accurate iteration of the calculated coupling constants is obtained. A listing of the *A* and *B* values along with some representative linear fits of the data are shown in the Supporting Information. In 1998, a new Karplus relationship based on J_{HF} coupling constants derived from a series of fluorinated nucleosides and conformationally biased molecules containing fluorine was derived and incorporated into the PSEUROT program[33] and later modified slightly by Mikhailopulo, et al.[16] Using our newly calculated *A* and *B* coefficients, we performed three sets of analyses: using (1) J_{HH} data alone, (2) J_{HF} data alone, or (3) both J_{HH} and J_{HF} data. These results are summarized in Table 5. We performed calculations using only J_{HH} data at 25 °C and expanded the calculations to use J_{HF} at two extreme temperatures (10 and 70 °C) to comprehensively explore the conformational space sampled by compounds **2**–**4**.

Several trends were apparent from the analysis of the pseudorotation data. It was obvious that all three analogues preferred two trans-disposed fluorine atoms, in agreement with solid-state

and ab initio data, arguing for two strong F–O4′GEs that overrode the tendency of other competing effects.[16] The inclusion of J_{HF} data only slightly altered the calculated pseudorotational equilibrium for compound **2**; however, some marked differences were seen for the *xylo*-disposed compounds **3** and **4**. The *arabino*-FF compound **2** preferred an *S* pucker with an *N*/*S* equilibrium of 0.14:0.86 and very low rmsd values at 25 °C. This was consistent with our previous work on monofluorinated adenosine[42] and uracil[39] derivatives. Inclusion of J_{HF} data where $v_{max}(N)$ was held constant at two separate values (38°and 46°) only resulted in minor differences in the calculated *P* value but an increase in the mole fraction of the minor *N* conformer (X_N between 0.18 and 0.21) was observed. Higher rmsd values for the calculated *J* values were also observed but these were not outside "accepted" ranges for PSEUROT calculations. More substantial differences were observed for xylosides **3** and **4** with inclusion of J_{HF}. Both of these compounds are heavily biased toward the *N* pucker with the X_N at unity for **3** and 89% for **4**, both with very low rmsd values for the calculated coupling constants, at 25 °C. Inclusion of J_{HF} tempers these values slightly, lowering X_N to 94% at 70 °C for compound **3** and between 80% and 76% for compound **4** at 10° and 70°, respectively. The P_N value moves toward the "east" in going from the uracil to the 6-azauracil base at 25 °C (P = 24.1° for **3**, P = 44.4° for **4**) but the inclusion of J_{HF} in the calculations results in similar values of P_N (P = 31.6° for **3**, P = 33.1°) for *xylo*-FF **4**. For xylosides **3** and **4**, the respective P_N values of 45.5°and 51.7°are very close to "eastern" puckers when only J_{HF} used in the calculations, but return more *N*-like (31.6°and 33.1°) when both J_{HH} and J_{HF} are employed. However, the X_S values are very similar when only J_{HF} or both the J_{HF} and J_{HH} data are used. These results along with the fact that the $v_{max}(N)$ values are significantly lower for 6-azauracil nucleoside **4** compared to uracil counterpart **3** may follow from the assumption that the repulsive interaction between the 3′-fluorine atom and the 6-nitrogen of the 6-azauridine effectively "flattens" the C3′ position of the furanose ring from an ^{3}E-type pucker to the $_4$E type. This in effect will relieve some of this repulsion by positioning the modified base in a more pseudoequatorial position while maintaining an *N* pucker. It might be expected that the 6-azauracil base, being more electronegative than uracil, should impart a stronger AE driving the pseudorotational equilibrium to remain the *N* pseudorotamer. The *S*-driving repulsive effect is, however, strong enough to "flip" the pucker to the southern hemisphere (X_S of 20% and 14% at 10 and 70 °C, respectively). It is noteworthy that 1-(2-deoxy-2-fluoro-β-D-arabinofuranosyl)-6-azauracil reveals very similar conformations in the solid state (P_N = 359.2°)[38,43] and in DMSO solution (P_N = 351.4°, $v_{max}(N)$ = 33.5°, X_N = 98%; I. A. Mikhailopulo, unpublished). A explanation for this "paradoxically" rigid structure of the 2′-"up" fluoro 6-azauracil derivative was put forth by Seela, et al.[38] as the favorable occupation of the N6 nitrogen in an intermediary position between the O4′ (2.906 Å) and pseudoequatorial fluorine atom at C2′ (2.762 Å).

Many of the conformational adjustments imparted by substitution of electronegative (or other) atoms into the furanose ring have been rationalized based on arguments relating to the anomeric[33] and gauche effects.[13,44] Recent reports[16-18] that studied similar difluorinated structures have invoked an alternate theory by Brunck and Weinhold[19] which suggest that, not only do vicinal electronegative atoms prefer a gauche arrangement, but the origins of this effect may more be due to an ap σ to σ^* stabilization when the donating bond is the least polar one and the acceptor orbital is at the most polarized bond. For compounds **2**–**4** with trans-disposed electronegative atoms, the analysis is simplified: Both effects, viz., either two strong GEs (F2′–O4′ and F3′–O4′) or two strong ap effects (H2′–O4′ and H3′–O4′), all present in all three molecules, appear to be responsible for keeping the ring puckers in the "preferred" orientation that one would predict on inspection of the structures. The AE seems to be a weak contributor to these structures. In addition, other ap effects (H1′–F2′ and F3′–C5′ for **2**, F3′–H4′ for **3** and **4**) contribute additional stabilization to the preferred structures.

Do any of our calculations speak to the aforementioned F3′–H6 attractive force described by Bergstrom?[21] The data described here suggests that this is operational in 3′-"up" fluoro pyrimidine nucleosides. The following lines of evidence lend credence to this proposal: (1) low-energy structures from high-level ab initio calculations position the 3′-fluorine atom and the H6 atom in compound **3** within H-bonding distance (2.3 Å); (2) the chemical shift of the 3′-fluorine atom in **3** is shifted upfield by nearly 3 ppm relative to the same signal in compound **4**; and (3) inclusion of J_{HF} information into the PSEUROT calculations yield data (nearly pure *N* pucker for **3**, flatter ring and higher proportion of X_S in **4** relative to **3**) that support this effect. Figure 6 shows the conformations of the ab intio calculated structures for compounds **3** and **4** supporting this hypothesis. This effect may be used in the future design of nucleosides to "hold" the χ angle in a high anti rotamer population.

Conclusions

We have rigorously defined the structures of three difluorouridine nucleosides by a variety of methods. We showed that the F–O4′ GE along with two strong H′–O4 ap effects are able to afford sugar puckers that agree with what would be predicted with two trans-disposed fluorine atoms, namely the two electronegative fluorines are pseudodiaxial in each analogue. The influence of the 6-azauracil base is evident form the calculated and experimental structures and the F3′–N6 repulsion gives rise to the remarkable population of the *S* pseudorotamer. This behavior of xyloside **4** is in contrast to the stereochemically "rigid" 1-(2-deoxy-2-fluoro-β-D-arabinofuranosyl)-6-azauracil in the solid state and in solution, as has been shown before by Seela et al.[38] The lack of anti-HIV activity in compound **2** could arise from either the added "rigidity" of having the two fluorines work in concert to keep the molecule in the *S* pucker, and/or an unfavorable electronic or steric arrangement for efficient phosphorylation of the 5′-hydroxyl group by cellular kinases. This work extends and greatly refines our previous work[20] and provides new insights that may be followed in designing new and (potentially) therapeutically useful nucleosides.

Supplementary Material

Refer to Web version on PubMed Central for supplementary material.

Acknowledgments

This research was supported in part by the Intramural Research Program of the NIH, National Cancer Institute, Center for Cancer Research. I.A.M. is thankful to the Alexander von Humboldt-Foundation (Bonn – Bad-Godesberg, Germany) and to the Foundation for the Basic Research (Belarus) for financial support.

References

1. Ismail FMD. J Fluorine Chem 2002;118:27–33.
2. Kirk KL, Filler R. Biomed Front Fluorine Chem 1996;639:1–24.
3. Park BK, Kitteringham NR, O'Neill PM. Annu ReV Pharmacol Toxicol 2001;41:443–470. [PubMed: 11264465]
4. Meng WD, Qing FL. Curr Top Med Chem 2006;6:1499–1528. [PubMed: 16918465]
5. Pankiewicz KW. Carbohydr Res 2000;327:87–105. [PubMed: 10968677]
6. Marquez VE, Tseng CKH, Mitsuya H, Aoki S, Kelley JA, Ford H, Roth JS, Broder S, Johns DG, Driscoll JS. J Med Chem 1990;33:978–985. [PubMed: 2106581]
7. Roth JS, McCully CM, Balis FM, Poplack DG, Kelley JA. Drug Metab Dispos 1999;27:1128–1132. [PubMed: 10497138]
8. Lodenosine Trial Halted. Aids Patient Care and Stds 2000;14:61.
9. Altona C, Sundaralingam M. J Am Chem Soc 1973;95:2333–2344. [PubMed: 4709237]

10. Vanroey P, Salerno JM, Chu CK, Schinazi RF. Proc Natl Acad Sci U S A 1989;86:3929–3933. [PubMed: 2726758]
11. Mirmehrabi M, Rohani S, Jennings MC. Acta Crystallogr Sect C: Cryst Struct Commun 2005;61:O695–O698.
12. Jagannadh B, Reddy DV, Kunwar AC. Biochem Biophys Res Commun 1991;179:386–391. [PubMed: 1883367]
13. Abraham RJ, Chambers EJ, Thomas WA. J Chem Soc Perkins Trans 1994;2:949–955.
14. Tavasli M, O'Hagan D, Pearson C, Petty MC. Chem Commun 2002:1226–1227.
15. Thibaudeau, C.; Acharya, P.; Chattopadhyaya, J. Stereoelectronic Effects in Nucleosides & Nucleotides and their Structural Implications. Vol. 2. Uppsala University Press; Uppsala, Sweden: 2005.
16. Mikhailopulo IA, Pricota TI, Sivets GG, Altona C. J Org Chem 2003;68:5897–5908. [PubMed: 12868924]
17. Sivets GG, Kalinichenko EN, Mikhailopulo IA. Lett Org Chem 2006;3:402–408.
18. Sivets GG, Kalinichenko EN, Mikhailopulo IA. HelV Chim Acta 2007;90:1818–1836.
19. Brunck TK, Weinhold F. J Am Chem Soc 1979;101:1700–1709.
20. Marquez, VE.; Lim, BB.; Barchi, JJ., Jr; Nicklaus, MC. Conformational Studies and Anti-HIV Activity of Mono- and Difluorodideoxy Nucleosides. Plenum Press; New York: 1993. p. 265-284.
21. Bergstrom DE, Swartling DJ, Wisor A, Hoffmann MR. Nucleosides Nucleotides 1991;10:693–697.
22. Martin JA, Bushnell DJ, Duncan IB, Dunsdon SJ, Hall MJ, Machin PJ, Merrett JH, Parkes KEB, Roberts NA, Thomas GJ, Galpin SA, Kinchington D. J Med Chem 1990;33:2137–2145. [PubMed: 2165161]
23. SMART and SAINT. Bruker AXS; Madison, WI: 1999.
24. Sheldrick, GM. SHELXS97 and SHELXL97. University of Göttingen; Göttingen, Germany: 1997.
25. Halgren TA. J Comput Chem 1996;17:490–519.
26. Qiu D, Shenkin PS, Hollinger FP, Still WC. J Phys Chem A 1997;101:3005–3014.
27. Chang G, Guida WC, Still WC. J Am Chem Soc 1989;111:4379–4386.
28. Frisch, MJ.; Trucks, GW.; Schlegel, HB. Gaussian 98. Gaussian, Inc.; Pittsburgh: 1998.
29. Wolinski K, Hinton JF, Pulay P. J Am Chem Soc 1990;112:8251–8260.
30. Kupce E, Freeman R. Chem Phys Lett 1996;250:523–527.
31. Kupce E, Boyd J, Campbell ID. J Magn Res, Ser B 1995;106:300–303.
32. Stott K, Stonehouse J, Keeler J, Hwang TL, Shaka AJ. J Am Chem Soc 1995;117:4199–4200.
33. Thibaudeau C, Plavec J, Chattopadhyaya J. J Org Chem 1998;63:4967–4984.
34. Plavec J, Tong WM, Chattopadhyaya J. J Am Chem Soc 1993;115:9734–9746.
35. Koole LH, Plavec J, Liu HY, Vincent BR, Dyson MR, Coe PL, Walker RT, Hardy GW, Rahim SG, Chattopadhyaya J. J Am Chem Soc 1992;114:9936–9943.
36. Thibaudeau C, Kumar A, Bekiroglu S, Matsuda A, Marquez VE, Chattopadhyaya J. J Org Chem 1998;63:5447–5462.
37. Watts JK, Sadalapure K, Choubdar N, Pinto BM, Damha MJ. J Org Chem 2006;73:921–925. [PubMed: 16438502]
38. Seela F, Chittepu P, He J, Eickmeier H. Acta Crystallogr, Sect C: Cryst Struct Commun 2004;60:O884–O886.
39. Barchi JJ, Jeong LS, Siddiqui MA, Marquez VE. J Biochem Biophys Methods 1997;34:11–29. [PubMed: 9089381]
40. Barchi JJ, Marquez VE, Driscoll JS, Ford H, Mitsuya H, Shirasaka T, Aoki S, Kelley JA. J Med Chem 1991;34:1647–1655. [PubMed: 2033591]
41. Wasylishen RE, Barfield M. J Am Chem Soc 1975;97:4545–4552.
42. Ford H, Dai F, Mu L, Siddiqui MA, Nicklaus MC, Anderson L, Marquez VE, Barchi JJ. Biochemistry 2000;39:2581–2592. [PubMed: 10704207]
43. Mikhailopulo IA, Sokolov YA, He JL, Chittepu P, Rosemeyer H, Seela F. Nucleosides Nucleotides Nucl Acids 2005;24:701–705.

44. Amos RD, Handy NC, Jones PG, Kirby AJ, Parker JK, Percy JM, Su MD. J Chem Soc, Perkins Trans 1992;2:549–558.

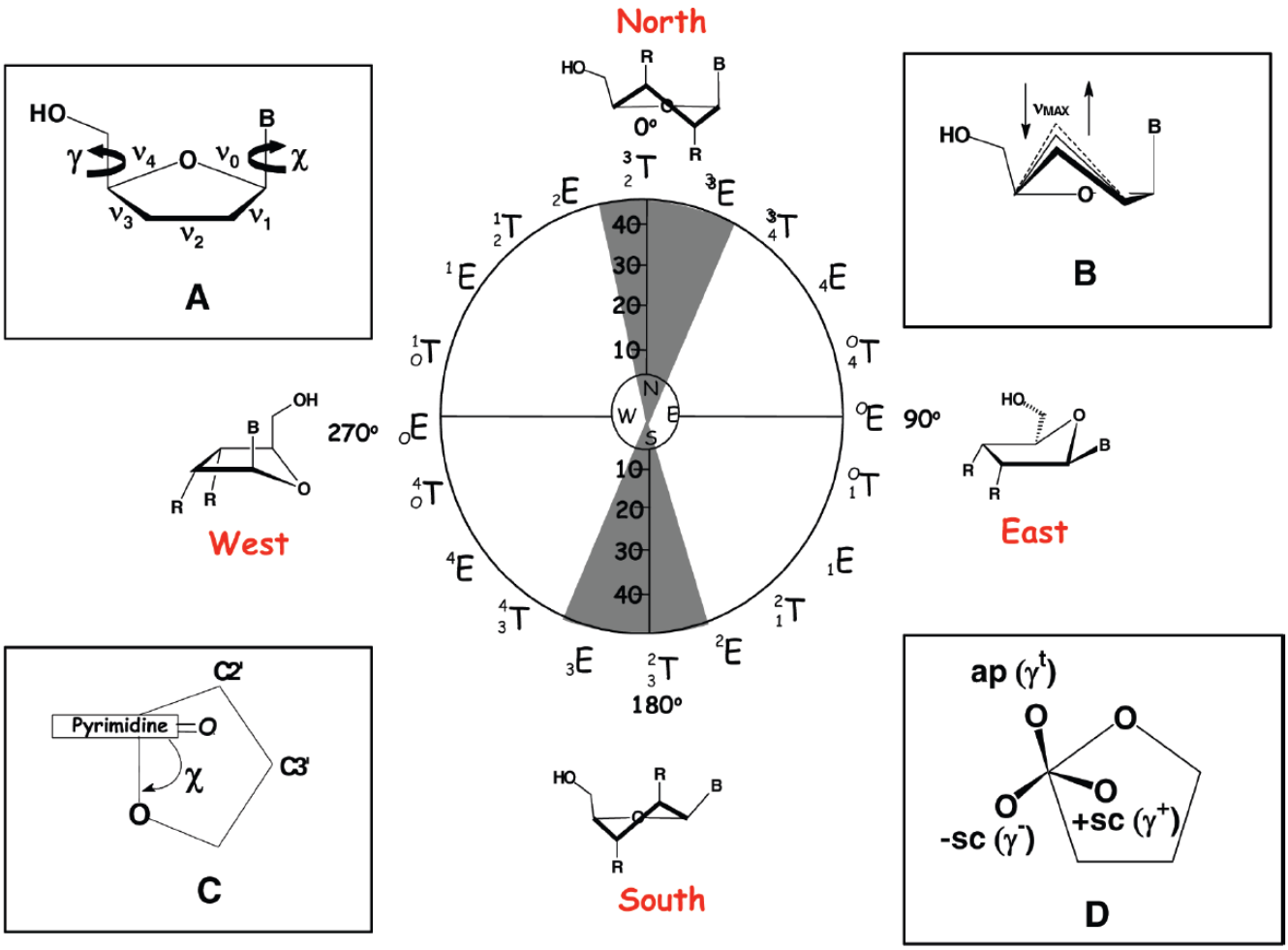

Figure 1.

Structural parameters for nucleosides. The pseudorotational cycle (center) describes the ring pucker of the furanose system where the endocyclic torsion angles (shown as v_0–v_4 in A) are varied systematically around a “wheel” of twist and envelope conformations. The maximum out-of-plane pucker (v_{max}, in B) indicates degree to which a specific atom in the five-membered ring will flex from the plane of the five atoms. Angles χ (C) and γ (D) describe the rotamer distribution about the anomeric and C4′–C5′ bonds, respectively.

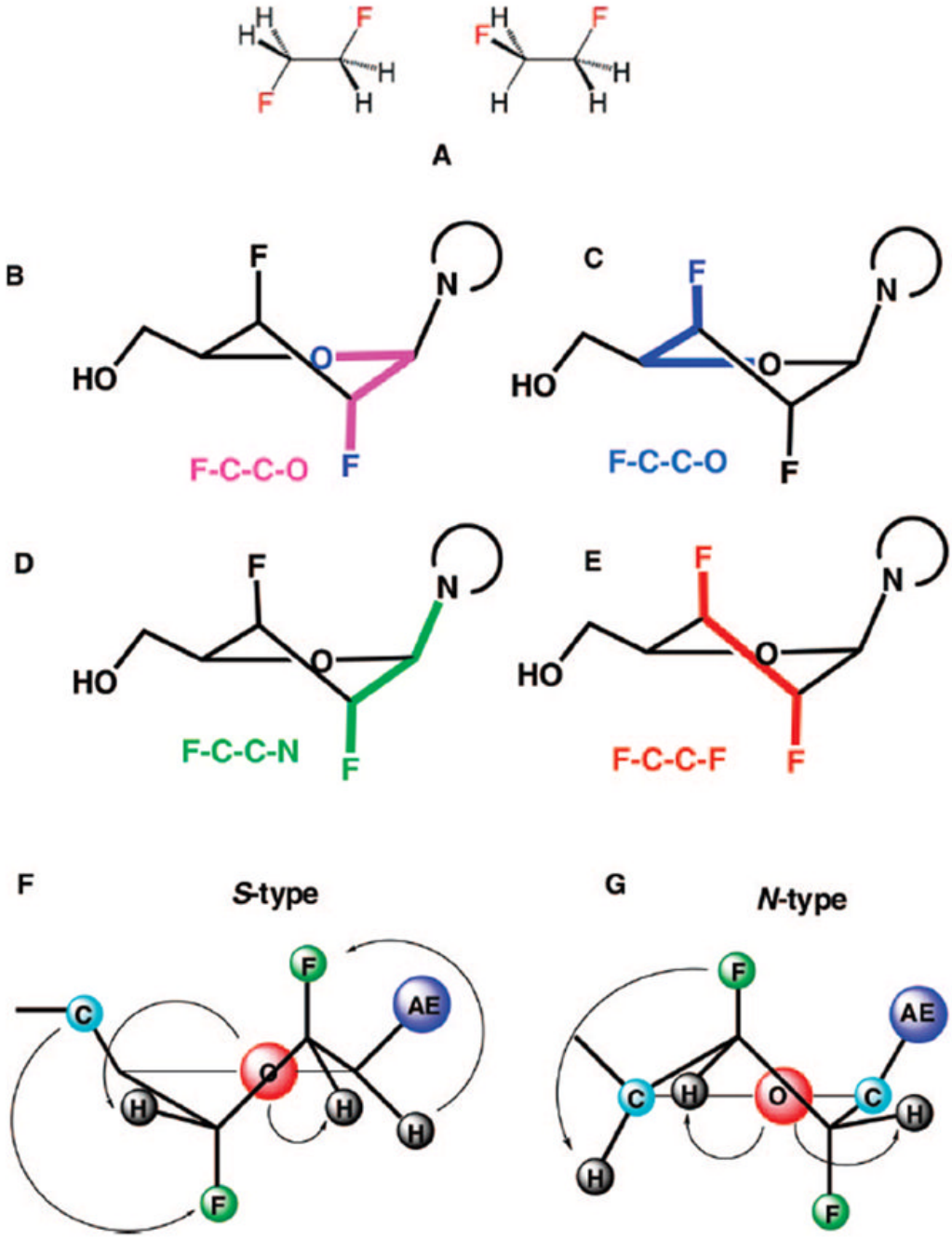

Figure 2.

Depiction of the gauche and antiperiplanar effects. In (A), the F atoms in difluoroethane can orient either antiperiplanar (left) or gauche (right). (B–E) Atoms involved in the potential gauche effects in the difluoronucleosides studied in this work; atoms involved are highlighted in bold. Potential antiperiplanar effects (depicted by arrows) for *S*-type (F) and *N*-type (G) puckers.

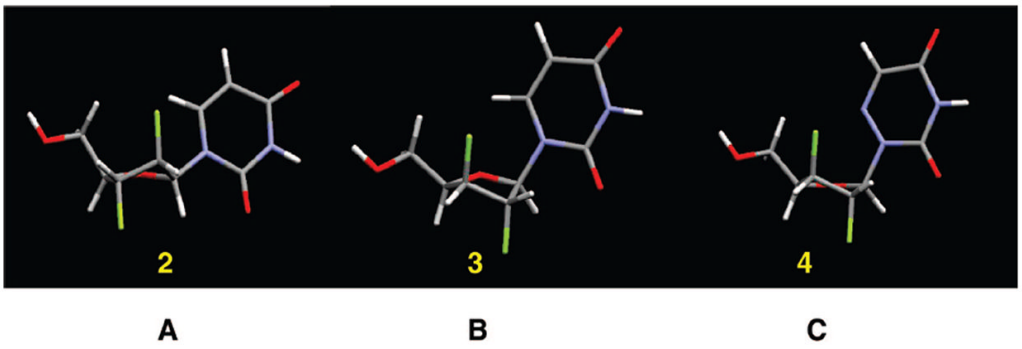

Figure 3.
Crystal structures of compounds (A) **2**, (B) **3**, and (C) **4**.

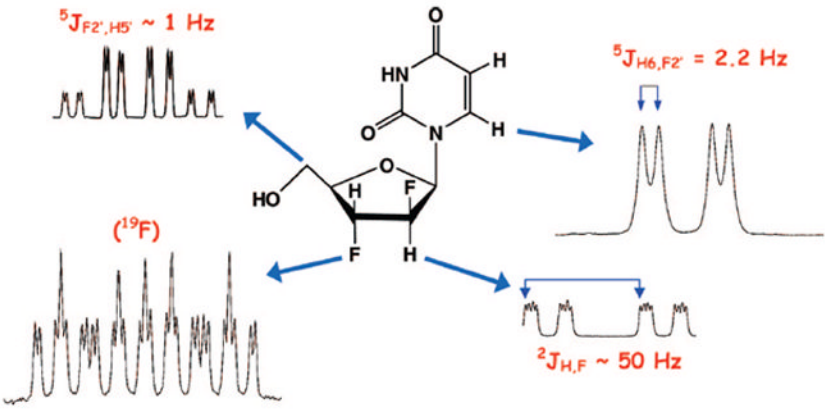

Figure 4.
Representative NMR resonances for compound **2**. The five-bond F2′–H6 interaction is shown in the upper right.

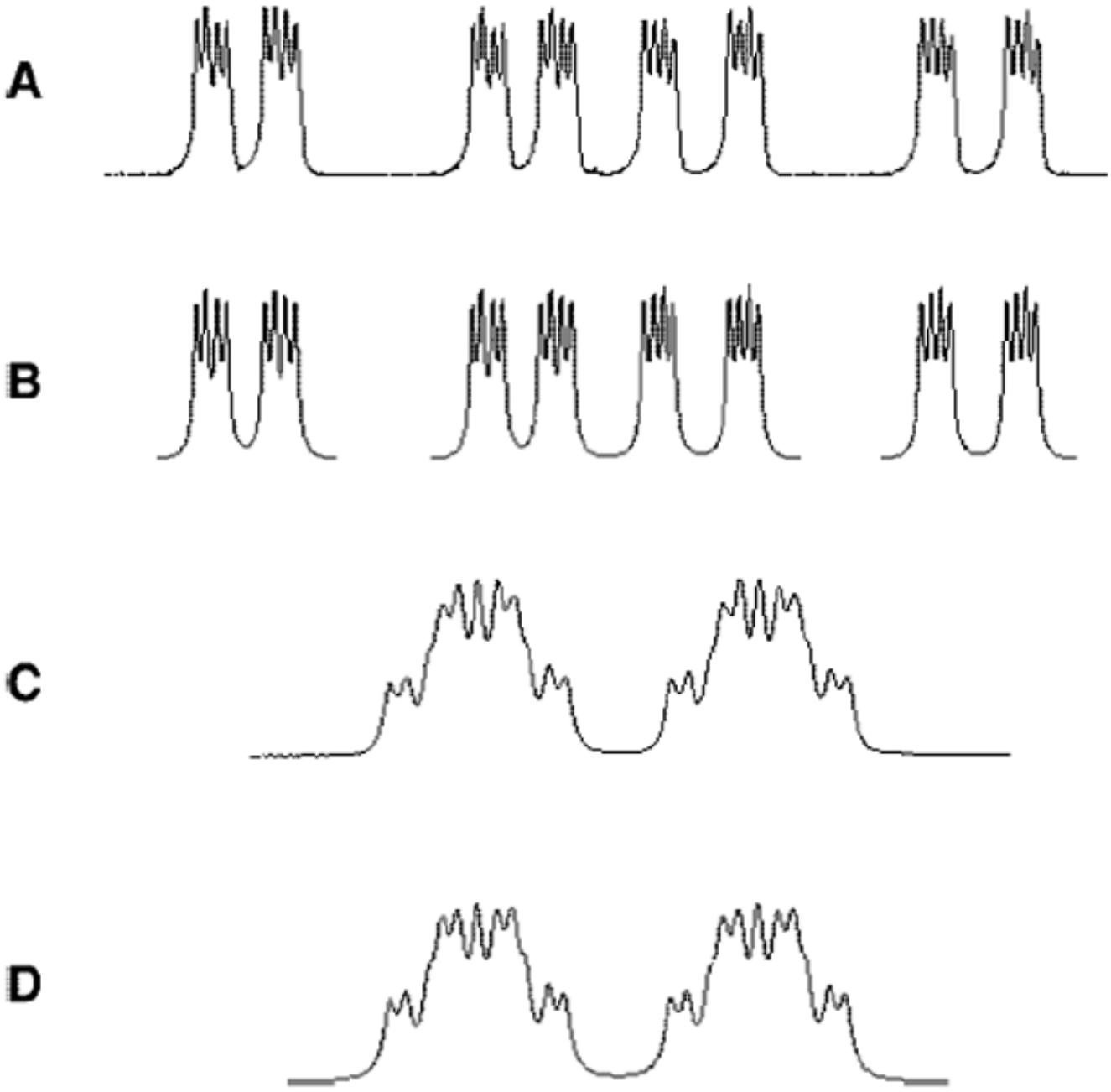

Figure 5.
Comparison of experimental (A and C) and simulated (B and D) multiplets for compound using gNMR for the simulation. Multiplets in A and B are the H2′ and H3′ from compound **2** at 10 °C. The multiplet in C and D is the H4′ proton of compound **4** at 25 °C.

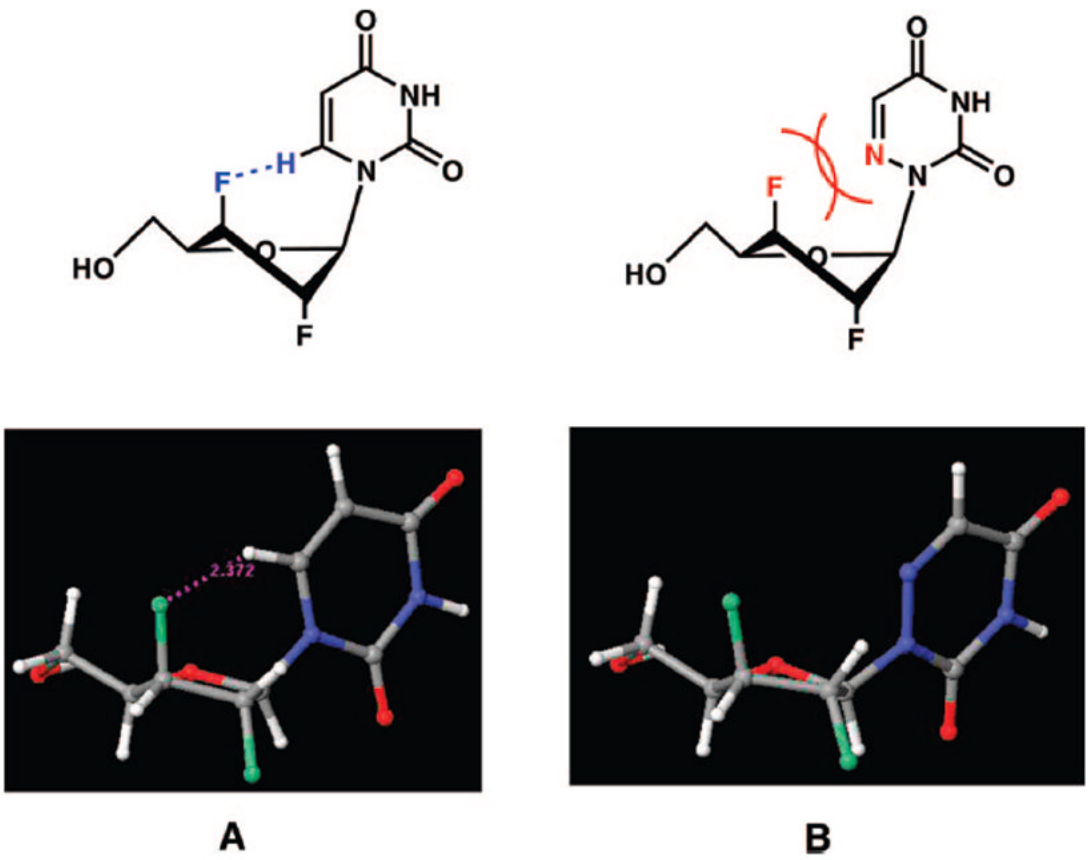

Figure 6.
Depiction of the F–H interaction/distance and the ab intio calculated structure for (A) compound **3** and (B) compound **4**. The distance from F3′ to H6 (2.372 Å) is shown with a dotted line in (A).

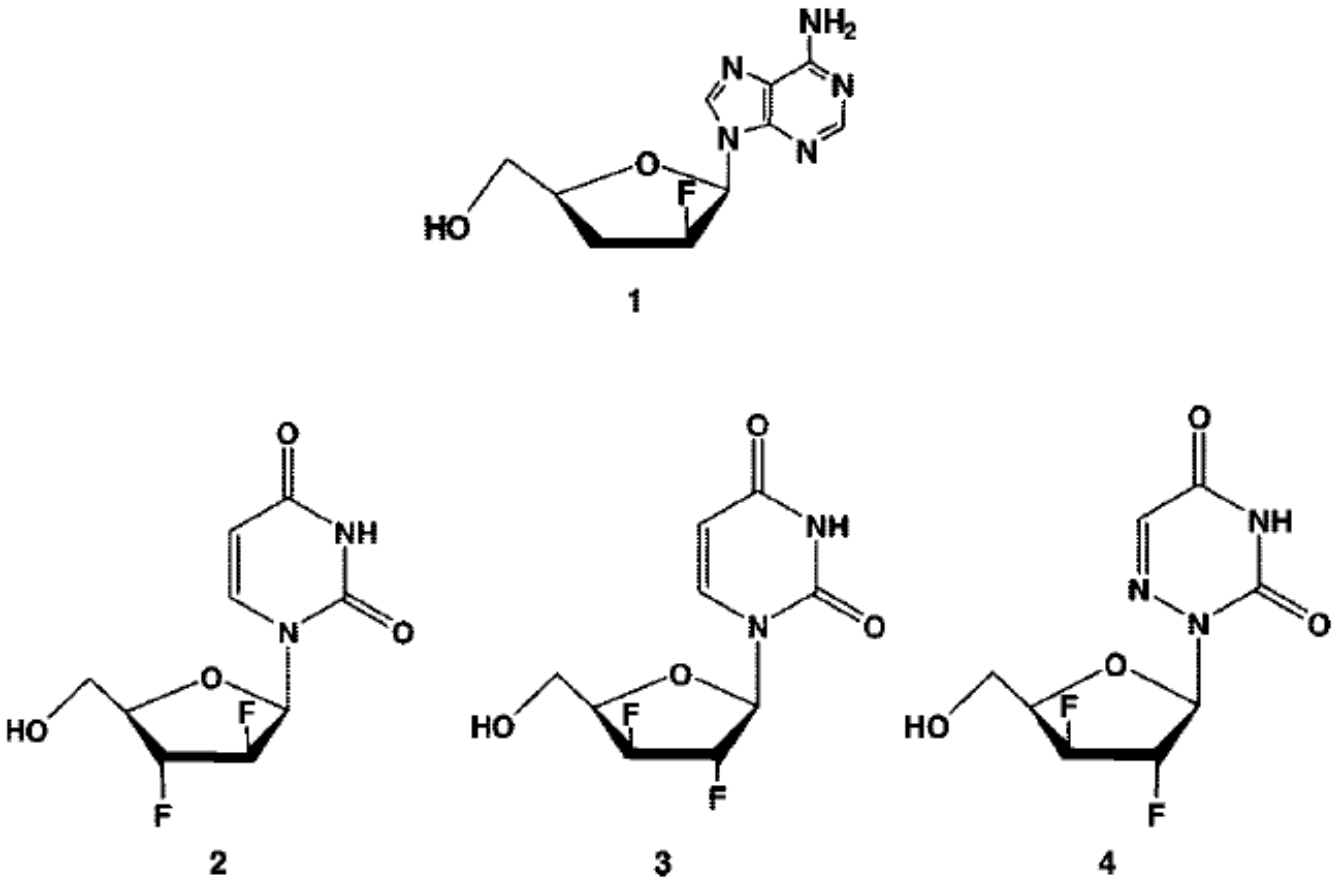

Chart 1.

Table 1

Conformational Parameters of Compounds **2**–**4** Calculated from X-ray Structures

compound	γ	χ	P	ν_m
2	−73.9(0.3) [a]	−142.8(0.2)	173.5(0.2)	30.5(0.1)
3a	178.3(0.3)	−160.0(0.2)	26.5(0.4)	32.6(0.1)
3b	−173.0(0.2)	−149.6(0.17)	11.9(0.21)	38.8(0.18)
3b′	−175.5(0.17)	−148.6(0.12)	58.0(0.17)	39.6(0.12)
4	−60.2(0.2)	−115.1(0.2)	55.0(0.2)	40.3(0.1)

[a] Numbers in parentheses are errors (estimated standard deviations) in degrees.

Table 2

Comparison of Nucleoside Structural Parameters for Compounds **2**–**4** as Determined from ab Intio Optimization and X-ray Crystallography

	ν_0	ν_1	ν_2	ν_3	ν_4	P^a	$\nu_{max}{}^a$	χ^a	γ^a	energy, hartrees (kcal/mol)[b]
araFF (**2**)										
X-ray	−12.77	26.85	−30.21	23.55	−6.76	174.29	30.36	−142.77	−74.07	
Conf 1	−36.93	36.64	−23.06	2.35	21.70	127.37	37.99	−133.53	179.83	−959.3580 (−602006.7585)
Conf 2	−29.85	36.78	−29.77	13.39	10.31	145.26	36.23	−136.03	−66.67	−959.3573 (−602006.2890)
xylFF (**3**)										
X-ray	−4.84	−15.95	29.55	−32.79	23.80	26.56	33.04	−159.95	178.17	
Conf 1	−19.40	−4.44	24.58	−36.42	35.59	48.99	37.45	−116.67	−176.87	−959.35850 (−602007.0533)
Conf 2	−19.53	−4.21	24.37	−36.29	35.57	49.30	37.37	−116.16	−176.87	−959.35853 (−602007.0747)
azxFF (**4**)										
X-ray	−24.73	0.03	23.10	−38.54	40.01	55.46	40.75	−115.09	−60.20	
Conf 1	−30.90	10.44	12.09	−30.43	38.91	71.42	37.94	−98.18	−176.46	−975.3722 (−612055.7746)
Conf 2	10.01	−26.54	31.75	−26.67	10.77	0.52	31.76	−159.77	63.03	−975.3680 (−612053.1466)

[a] Calculated with the online pseudorotation tool at http://cactus.nci.nih.gov/Pseurot.

[b] Optimization was at the B3LYP/6-311++G**Opt level of theory in Gaussian98.

Table 3

H–H Coupling Constant Values (in Hz) at Two Extreme Temperatures for Compounds **2**–**4**

	T(K)	$J_{1',2'}$	$J_{2',3'}$	$J_{3',4'}$	$J_{4',5'}$	$J_{4',5''}$	$J_{5',5''}$
2	283	3.57	1.63	3.33	4.40	6.10	−12.50
	343	3.76	1.72	3.48	4.41	6.10	−12.46
3	283	1.07	1.05	2.58	4.91	6.85	−12.26
	343	1.65	1.18	2.69	5.09	6.57	−12.30
4	283	2.83	0.88	3.77	4.81	6.90	−12.11
	343	2.89	1.28	4.02	4.98	6.98	−12.12

J Am Chem Soc. Author manuscript; available in PMC 2009 September 8.

Table 4

H–F and F–F Coupling Constant Values (in Hz) at Two Extreme Temperatures for Compounds **2**–**4**

	T(K)	$J_{H1',F2'}$	$J_{H2',F2'}$	$J_{F2',H3'}$	$J_{H2',F3'}$	$J_{H3',F3'}$	$J_{F3',H4'}$	$J_{F2',H4'}$	$J_{F3',H1'}$	$J_{F,H5(H5'')}$	$J_{F2',H6}$	J_{FF}
2	283	19.90	49.58	14.9	11.73	49.80	26.00	0.95	2.22	0.80	2.00	9.35
	343	19.28	49.73	14.83	11.98	49.95	25.74	0.95	2.06	*a*	2.29	*a*
3	283	19.78	47.21	8.44	10.96	49.00	31.64	3.09		0.95		11.93
	343	19.85	47.18	9.13	11.83	48.92	31.31	3.11		1.28		*a*
4	283	21.72	48.85	13.10	15.57	50.34	27.39	1.64				8.24
	343	21.28	48.88	13.62	15.74	50.43	26.97	1.62				*a*

[a]Not calculated due to broadened spectrum at 70 °C.

Table 5

PSEUROT Data for Compounds **2**–**4**

compound	temp (°C)	P_N	ν_{max}(N)	P_S	ν_{max}(S)	rmsd (Hz)	|ΔJ| (Hz)	X_N (%)
2[a]		0.0[b]	34.0[b]	137	32.6	0.0	0.0	14
[H,H]	10	29.0	38[b]	132.6	34.0	0.027	0.04	19
	70					0.027	0.04	21
[H,F]	10	20.1	38[b]	134.2	35.2	0.052	0.07	18
	70					0.079	0.12	21
[H,H and H,F] [c]	10	23.3	38[b]	133.3	35.2	0.101	[HH] 0.10 [HF] 0.23	18
	70					0.133	[HH] 0.17 [HF] 0.28	21
[H,H and H,F][d]	10	19.6	38[b]	132.6	36.0	0.091	[HH] 0.14 [HF] 0.12	18
	70					0.125	[HH] 0.22 [HF] 0.13	21
3[a]		24.1	33.4	160[b]	34[b]	0.179	0.18	100
[H,H]	10	31.2	33.1	85[b]	38[b]	0.093	0.183	100
	70					0.104	0.051	94
[H,F]	10	45.5	42.0	143.2	38[b]	0.236	0.33	94
	70					0.258	0.38	91
[H,H and H,F]	10	31.6	33.7	100.3	38[b]	0.190	[HH] 0.23 [HF] 0.22	100
	70					0.077	[HH] 0.09 [HF] 0.15	94
4[a]		44.4	27.7	150[b]	38[b]	0.0	0.00	89
[H,H]	10	40.9	26.2	144[b]	38[b]	0.089	0.10	89
	70					0.092	0.11	85
[H,F]	10	51.7	38.3	127.0	38[b]	0.118	0.21	75
	70					0.078	0.12	71
[H,H and H,F][c]	10	33.1	28.7	112.3	38[b]	0.092	[HH] 0.10 [HF] 0.25	80

J Am Chem Soc. Author manuscript; available in PMC 2009 September 8.

compound	temp (°C)	P_N	ν_{max}(N)	P_S	ν_{max}(S)	rmsd (Hz)	$\|\Delta J\|$ (Hz)	X_N (%)
	70					0.191	[HH] 0.21	76
							[HF] 0.23	
[H,H and H,F] [d]	10	36.8	31.2	113.8	38[b]	0.102	[HH] 0.16	79
							[HF] 0.08	
	70					0.203	[HH] 0.34	74
							[HF] 0.16	

[a] PSEUROT performed with the MANY option at one temperature (25 °C).

[b] Values held constant during the calculations.

[c] Scale factors of 1.0 and 0.2 for HH and HF, respectively.

[d] Equal Scale factors of 1.0 for both HH and HF.